AIAA-2000-4281

GENERIC NEURAL FLIGHT CONTROL AND AUTOPILOT SYSTEM

John Kaneshige*, John Bull† and Joseph J. Totah‡

Abstract

This paper describes a generic neural flight control and autopilot system, which can be applied to a wide range of vehicle classes. A neural flight control system is used to provide adaptive flight control, without requiring extensive gain-scheduling or explicit system identification. The neural flight control system uses reference models to specify desired handling qualities, and can receive commands from a generic guidance system to provide outer-loop autopilot control. The generic guidance system performs automatic gain-scheduling using frequency separation, based upon the neural flight control system's specified reference models. A variety of different aircraft were examined to ensure applicability to multiple vehicle classes including commercial transports, high performance military aircraft, and hypersonic concepts. Simulation results are presented for a mid-sized twin-engine commercial jet transport concept, a modified F-15 with moveable canards attached to the airframe, and a small single-engine uninhabited aerial vehicle hypersonic "waverider" concept. Results demonstrate that the generic neural flight control and autopilot system can achieve performance comparable to each aircraft's respective conventional system, while providing additional potential for accommodating damage or failures.

Introduction

Over the last 50 years, aircraft avionics have evolved from basic electrical systems to highly advanced flight and vehicle management systems. However, these technological advances have also resulted in a dramatic increase in the costs associated with avionics development, from approximately 4% of the flyaway cost for a World War II fighter, to about 56% for America's highly advanced F-22 Raptor.[1]

A portion of the cost associated with avionics can be attributed to control law development. With the advent of fly-by-wire flight control technology, it has become possible to shape the handling qualities of an aircraft to desired specifications, even when applied to unstable aircraft designs. Most conventional flight control systems utilize extensive gain-scheduling in order to achieve desired handling qualities. While this approach has proven to be very successful, the development process can be expensive and often results in aircraft specific implementations. Over the past several years, various adaptive control techniques have been investigated.[2]

A neural network based approach, incorporating direct adaptive control with dynamic inversion[3], was selected in order to develop a generic flight control system capable of providing consistent handling qualities without requiring extensive gain-scheduling or explicit system identification. This particular architecture uses both pre-trained and on-line learning neural networks, and reference models to specify desired handling qualities. Pre-trained neural networks are used to provide estimates of aerodynamic stability and control characteristics required for model inversion. On-line learning neural networks are used to compensate for errors and adapt to changes in aircraft dynamics. As a result, consistent handling qualities can be achieved across flight conditions and for different aircraft configurations. The architecture remains the same for different aircraft applications, requiring only the pre-training of neural networks and the specification of desired handling quality reference models. An Integrated Vehicle Modeling Environment (IVME)[4], which incorporates vortex-lattice code with a rapid aircraft modeler, is used to estimates aerodynamic stability and control characteristics for pre-training neural networks.

A generic guidance system is used to provide autopilot control or pilot feedback through a flight director. This commercial aircraft based guidance system takes advantage of the consistent handling qualities provided by the neural flight control system. Automatic gain-scheduling is performed by using frequency separation, based upon the neural flight control system's specified reference models.

Simulation evaluations were performed on a variety of different aircraft to ensure applicability to a wide range of vehicle classes including commercial transports, high performance military aircraft, and

* Computer Engineer, Member AIAA, NASA Ames Research Center, Moffett Field, CA

† Consultant, Member AIAA, QSS Group, Inc., Moffett Field, CA

‡ Aerospace Engineer, Associate Fellow AIAA, NASA Ames Research Center, Moffett Field, CA

hypersonic concepts. High fidelity aerodynamic models were supplied for the simulated aircraft described below:

- Lockheed Georgia Company's commercial transport concept, developed as a simulation in 1983,
- NASA Dryden's F-15 ACTIVE aircraft, equipped with canards and thrust vectoring nozzels, and
- Accurate Automation Corporation's LoFLYTE™ uninhabited aerial vehicle (UAV), developed as a hypersonic "waverider" concept.

This paper contains a brief overview of the neural flight control and generic autopilot systems, and presents simulation results comparing their performance to each aircraft's respective conventional systems. Piloted simulations were performed on the Advanced Concepts Flight Simulator (ACFS)[5] at NASA Ames Research Center.

Neural Flight Control System

The neural flight control architecture is based upon the augmented model inversion controller, developed by Rysdyk and Calise.[3] This direct adaptive tracking controller integrates feedback linearization theory with both pre-trained and on-line learning neural networks. Pre-trained neural networks are used to provide estimates of aerodynamic stability and control characteristics required for model inversion. On-line learning neural networks are used to generate command augmentation signals to compensate for errors in the estimates and from the model inversion. The on-line learning neural networks also provide additional potential for adapting to changes in aircraft dynamics due to damage or failure. Reference models are used to filter command inputs in order to specify desired handling qualities. A Lyapunov stability proof guarantees boundedness of the tracking error and network weights.[3]

Figure 1 contains a diagram of the neural flight control system. Commands are generated by the pilot through lateral and longitudinal stick and rudder pedal displacements (*dla*, *dln*, *dpd*). Turn coordination is provided through the suppression of lateral acceleration (*ny*). Stick and rudder pedal gains (*Kla*, *Kln*, *Kpd*) are used to convert displacement commands into roll rate, and aerodynamic normal and lateral acceleration commands (p_{cmd}, nz_{cmd}, ny_{cmd}). These commands are then transformed into corresponding roll rate, pitch rate, and yaw rate commands (p_{com}, q_{com}, r_{com}). Reference models are used to generate filtered rate commands (p_c, q_c, r_c) and acceleration commands (p'_c, q'_c, r'_c). Dynamic inversion is used to compute the necessary control surface deflections (*dail*, *dtail*, *stab*, *elev*, *drud*, *dcan*). Adaptive neural networks use aircraft state information (*Xp*, *Xq*, *Xr*) to generate pseudo control augmentation commands (Up_{ad}, Uq_{ad}, Ur_{ad}) in order to compensate for errors (p_e, q_e, r_e) computed from aircraft feedback (*p*, *q*, *r*).

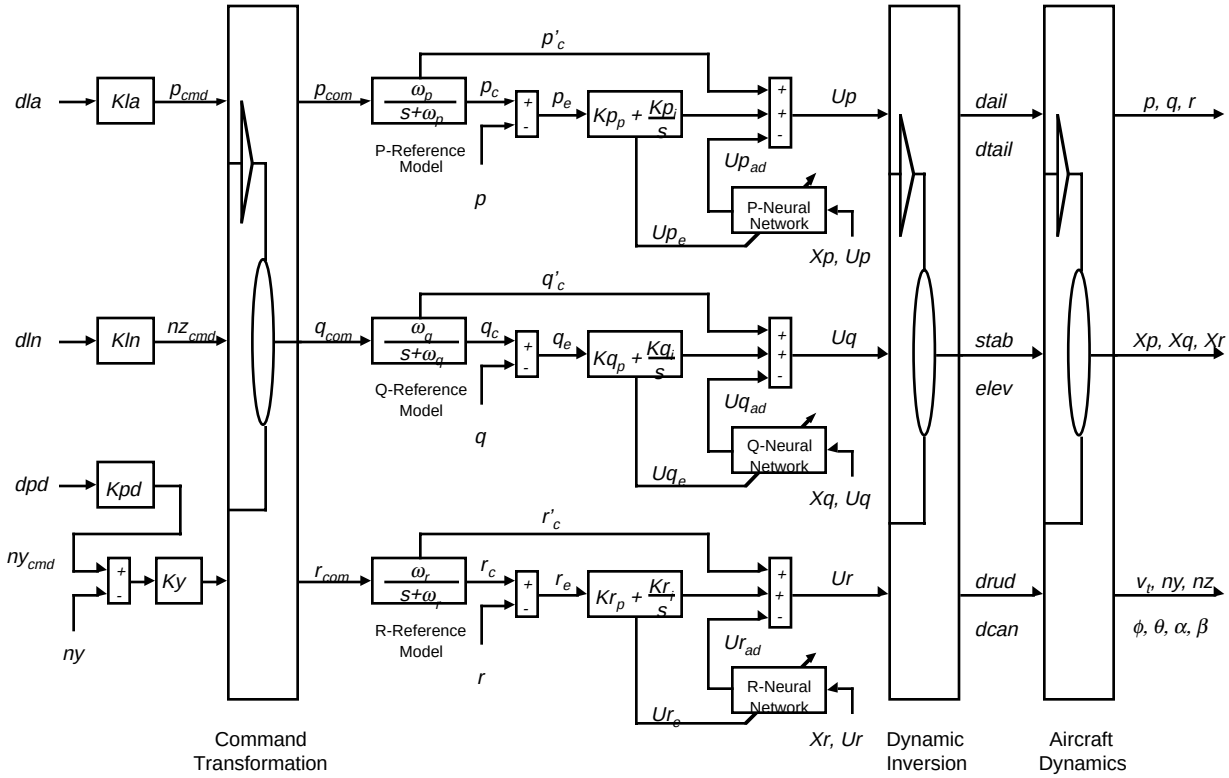

Figure 1. Neural Flight Control System

Reference Models

The reference models used for this evaluation consisted of first-order roll rate, pitch rate and yaw rate transfer functions with a DC gain of one. Table 1 contains the reference model frequencies (ω_p, ω_q, ω_r) that were used for each aircraft. Alternate reference models can be applied to specify different handling qualities for each aircraft. Reference model scheduling can also be applied in order to accommodate performance limitations at different flight conditions.

Table 1. Aircraft Reference Model Frequencies

Frequency	Transport	F-15	UAV
ω_p	3.5	5.0	4.2
ω_q	2.5	3.8	3.1
ω_r	2.0	3.0	1.5

A design criteria is used for computing stick and rudder pedal gains, which is based on desired roll rate, and aerodynamic normal and lateral acceleration command limits (p_{max}, nz_{max}, ny_{max}). Table 2 contains the design criteria parameters used to compute stick and rudder pedal gains for each aircraft.

$$Kla = p_{max} / dla_{max} \tag{1}$$

$$Kln = \frac{g}{v_t}\left(nz_{max} / dln_{max}\right) \tag{2}$$

$$Kpd = \frac{g}{v_t}\left(ny_{max} / dpd_{max}\right) \tag{3}$$

The longitudinal stick and rudder pedal gains are scheduled on true airspeed (v_t) and also incorporates the acceleration of gravity (g).

Table 2. Aircraft Design Criteria Parameters

Limits	Transport	F-15	UAV
p_{max}	0.28	2.00	0.72
nz_{max}	1.12	7.2	1.68
ny_{max}	0.16	1.2	0.48

Command Transformation

Transformations can be used to convert normal and lateral aerodynamic acceleration commands into body-axis pitch rate and yaw rate commands.[6] These relationships can be expressed as

$$q = \frac{g_0}{u} nz - \frac{g\cos\phi\cos\theta - vp - \dot{w}}{u} \tag{4}$$

$$r = \frac{g_0}{u} ny + \frac{\dot{v} - wp - g\sin\phi\cos\theta}{u} \tag{5}$$

The scaling factor (g_0) is used for converting accelerations to g's.

While sensors can provide pitch and bank angle measurements (θ, ϕ), translational velocities (u, v, w) and accelerations ($\dot{v}$, $\dot{w}$) are normally not available, As a result, the command transformations are approximated by

$$q_{com} = \frac{g}{v_t} nz_{cmd} + \frac{v_g}{v_t} p\sin\beta \tag{6}$$

$$r_{com} = \frac{g}{v_t}\left(ny_{cmd} + \sin\phi\cos\theta\right) + p\tan\alpha \tag{7}$$

Estimated values are used for angle-of-attack (α), sideslip (β), and ground speed (v_g). The elimination of the term $\{(g/g_0)\cos\phi\cos\theta\}$ causes the definition of the normal acceleration command to exclude the force necessary to compensate for the aircraft's orientation with respect to gravity. Additional terms for providing level-turn compensation can be applied for aircraft that are limited to small bank angle operations.

Normal and lateral acceleration feedback can be applied in order to compensate for errors in the command transformation approximation. However, the overall handling qualities would be affected by the slower frequencies required for outer-loop control. As a result, feedback is not incorporated into the normal acceleration command in order to maximize the frequency response in the longitudinal axis. However, feedback is incorporated into the lateral acceleration command in order to minimize any adverse yaw buildup.[6]

$$n\hat{y}_{cmd} = Ky\,(ny_{cmd} - ny) \tag{8}$$

$$Ky = \frac{v_t m}{\bar{q} S \hat{C}y_\beta} \frac{\omega_r}{3} \tag{9}$$

Frequency separation is used to ensure that the outer-loop lateral acceleration control will not interfere with the inner-loop yaw rate control.

Dynamic Inversion

Dynamic inversion is based upon feedback linearization theory. No gain-scheduling is required since gains are functions of aerodynamic stability and control derivative estimates and sensor feedback. A Levenberg-Marquardt (LM) multi-layer perceptron[7] is used to provide dynamic estimates for model inversion. The LM network was pre-trained with stability and control derivative data generated by the IVME vortex-lattice code. In general, derivative estimates were achieved to within 10% of their actual values.[4]

To perform the model inversion, acceleration commands are used to replace the actual accelerations in the quasi-linear model

$$\begin{bmatrix} \dot{p} \\ \dot{q} \\ \dot{r} \end{bmatrix} = A(x)\begin{bmatrix} p \\ q \\ r \end{bmatrix} + B\begin{bmatrix} \delta_{lat} \\ \delta_{lon} \\ \delta_{dir} \end{bmatrix} \quad (10)$$

The model is then inverted in order to solve for the necessary control surface positions.

$$\begin{bmatrix} \delta_{lat} \\ \delta_{lon} \\ \delta_{dir} \end{bmatrix} = B^{-1}\left\{\begin{bmatrix} U_p \\ U_q \\ U_r \end{bmatrix} - A(x)\begin{bmatrix} p \\ q \\ r \end{bmatrix}\right\} \quad (11)$$

For aircraft equipped with redundant control surfaces, control allocation is handled by blending control surfaces according to desired specifications. Table 3 contains the control surface blending for each aircraft.

Table 3. Control Surface Blending

	Transport	F-15	UAV
δ_{lat}	*dail*	*dtail* = 2*dail*	*dtail*
δ_{lon}	*elev*	*stab*	*stab*
δ_{dir}	*drud*	*drud* = -*dcan*	*drud*

For the F-15 ACTIVE aircraft, symmetric canards (*can*) were scheduled with angle-of-attack and controlled independently.

Error Handling

If dynamic inversion and aircraft dynamics behaved as a perfect integrator for each of the three axes, then the closed-loop systems would be identical to their corresponding reference models. However, errors are introduced due to inaccuracies in the derivative estimates and from the model inversion. In order to achieve a rate-command-attitude-hold (RCAH) system, error handling is used to correct for errors detected from roll rate, pitch rate, and yaw rate feedback. The error dynamics, defined by proportional and integral (PI) gains, must be fast enough to track the reference models, yet slow enough to not interfere with actuator dynamics.

In order to ensure low-gain error handling performance, the error handling system is designed with natural frequencies (ω_n) that match the reference model frequencies, and with damping ratios (ζ) of $1/\sqrt{2}$. These frequencies and damping ratios are reflected in the PI gains.

$$K_p = 2\zeta\omega_n \quad (12)$$

$$K_i = \omega_n^{\,2} \quad (13)$$

If dynamic inversion and aircraft dynamics behaved as a perfect integrator for each of the three axes, then the resulting closed-loop error handing system would be

$$\frac{Y(s)}{X_c(s)} = \frac{s+\omega_n^2}{s^2+2\zeta\omega_n s+\omega_n^2} \quad (14)$$

Adaptive Neural Networks

The adaptive neural networks work in conjunction with the error handling system. By recognizing patterns in the behavior of the error, the neural networks can learn to remove biases through control augmentation commands. This allows the integrators to operate at nominal levels, without having to windup to remove error biases. This allows the neural flight control system to provide consistent handling qualities.

A two-layer sigma-pi neural network is used for each channel.[3] Inputs into the network consist of control commands, sensor feedback, and bias terms. Table 4 contains the inputs for each input signal category. Normalized inputs for the aircraft's altitude (*h)* and airspeed are used in the first category of inputs, to compensate for dynamic pressure effects.

Table 4. Input Signal Category Elements

	P-Network	Q-Network	R-Network
C_1	.1, v_t, v_t^2, h	.1, v_t, v_t^2, h	.1, v_t, v_t^2, h
C_2	.1, r, p, p_c, $\frac{1-e^{-(Up-Up_{ad})}}{1+e^{-(Up-Up_{ad})}}$	.1, q, q_c, $\frac{1-e^{-(Uq-Uq_{ad})}}{1+e^{-(Uq-Uq_{ad})}}$	.1, p, r, r_c, $\frac{1-e^{-(Ur-Ur_{ad})}}{1+e^{-(Ur-Ur_{ad})}}$
C_3	.1, α, β	.1, α, β	.1, α, β

The output of the neural network is the control augmentation command.

$$U_{AD} = W^T B(C_1, C_2, C_3) \quad (15)$$

The vector of basis functions (*B*) is computed from the inputs in each signal category using a nested kronecker product. The network weights (*W*) are computed by an adaptation law, which incorporates an adaptation gain (*G*) and deadband (*L*), and the command augmentation error (U_e) computed by the error handling system.[3]

$$\dot{W} = -G\left(U_e B + L|U_e|W\right) \quad (16)$$

$$U_e = \frac{1}{2K_i}\int e + \frac{1+K_i}{2K_iK_p}e \quad (17)$$

The adaptation gains and deadbands used for this evaluation were 18500 and 0.1 respectively.

Windup Protection

Windup protection is incorporated to prevent integrators and neural networks from trying to compensate for errors during control saturation. Windup

protection is activated when an actuator is commanded beyond its limit, causing the loss of control on one axis.

When windup protection is activated, the corresponding integrator becomes limited at its current value. Adaptation for the corresponding neural network is also turned off, by setting the adaptation gain to zero. To prevent to propagation of error during dynamic inversion, the saturated control axis is essentially removed from the B-matrix. The saturated actuators become effectively modeled as part of the plant.

Generic Autopilot System

Guidance systems used in commercial aircraft can provide outer-loop autopilot control or pilot feedback through a flight director. Most conventional guidance systems utilize a gain-scheduling approach, which is dependent upon the inner-loop performance of the flight control system. The generic guidance system uses a similar approach, however takes advantage of the neural flight control system's characteristic of providing consistent handling qualities. Automatic gain-scheduling is performed, using frequency separation, based on the neural flight control system's specified reference models.

Figure 2 contains a diagram of the generic autopilot concept. The pilot interface is through the mode control panel (MCP). The mode processor determines flight mode and target information, which is used by the guidance control laws, to generate flightpath angle (FPA) and bank angle commands. Automatic gain scheduling is performed to ensure that outer-loop guidance control does not interfere with the inner-loop flight control dynamics. When the autopilot is engaged, commands are transformed into body-axis rate commands and sent to the neural flight control system. When the autopilot is not engaged, graphical feedback may be provided through the flight director.

Since the neural flight controller has the ability to adapt, the generic guidance system does not have to rely on the use of integrators, in order to compensate for error biases. This allows the same control laws to be used for both the autopilot and flight director systems. Previous research has shown that conventional flight director systems, may encounter difficulty compensating for errors due to asymmetries caused by unexpected damage or failures.[8]

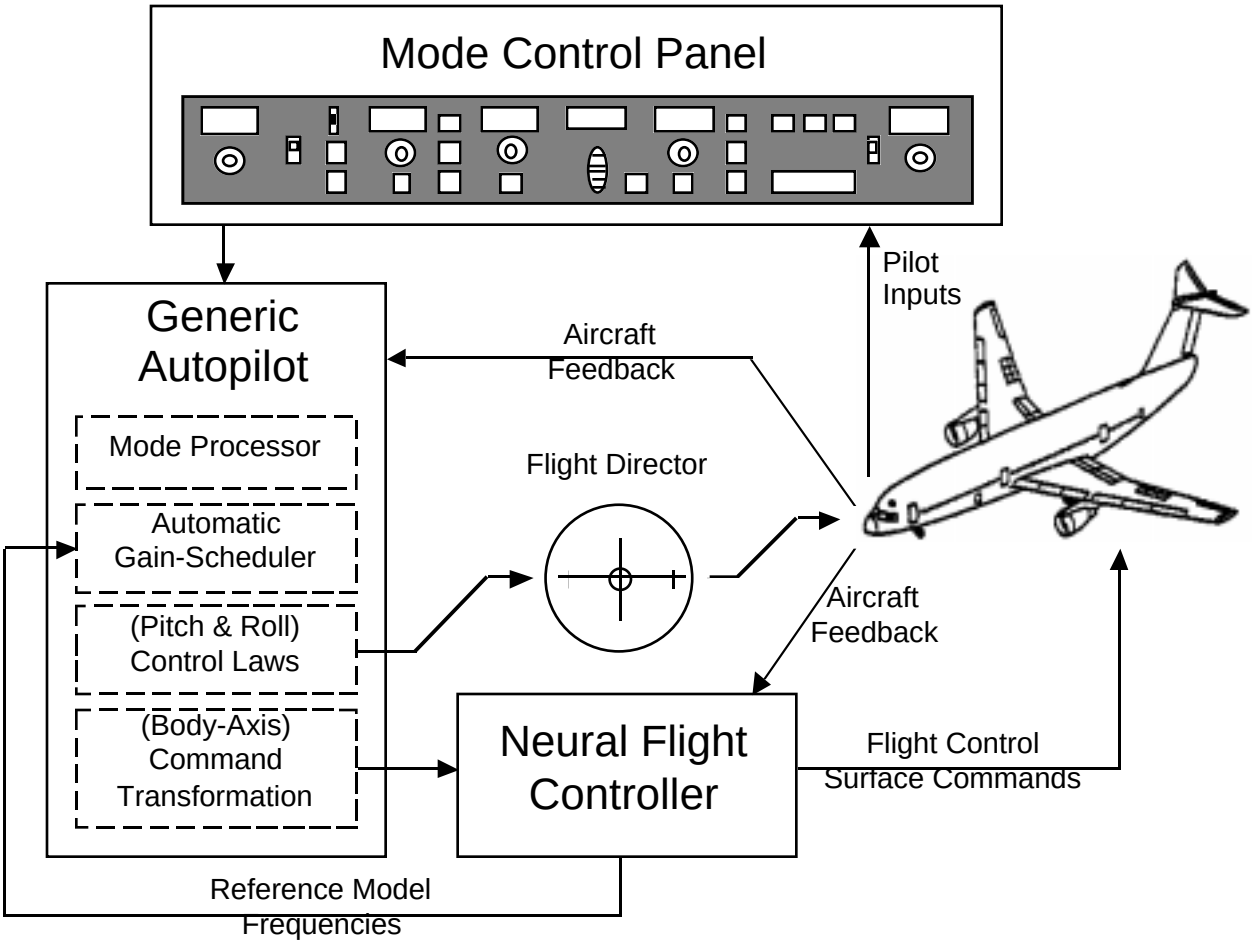

Figure 2. Generic Autopilot Concept

Mode Processor

The mode processor receives inputs from the MCP and generates longitudinal and lateral guidance modes and targets. Table 5 contains a list of the modes supported for this evaluation.

Table 5. Supported Flight Modes

Longitudinal Modes	Lateral Modes
FPA Select	Bank Select
Vertical Speed	Heading/Track Select
Altitude Capture/Hold	Heading/Track Hold
Glideslope Capture/Tracking	Localizer Capture/Tracking
Flare	

Automatic Gain-Scheduler

The automatic gain-scheduler computes all guidance control gains using a combination of inputs from the neural flight control system, sensor feedback, and design criteria specified constants. Frequency separation, based upon the neural flight control system's reference models, is used to ensure that outer-loop guidance dynamics are slow enough to avoid interference with inner-loop flight control.

A maximum FPA command (γ_{max}) can be specified, or computed as a function of stall limits. A maximum bank angle command (ϕ_{max}), can also be specified, or selected from the bank limit selector on the MCP. The FPA and bank command limits used for this evaluation correspond to 30 degrees and 10 degrees respectively.

Pitch and roll rate command limits are specified in terms of percent stick deflections.

$$\dot{\theta}_{max} = 25\% \left(\frac{g}{v_t} nz_{max} \right) \tag{18}$$

$$\dot{\phi}_{max} = 25\% \left(p_{max} \right) \tag{19}$$

The maximum bank angle command is used to limit the corresponding heading (or track) rate command.

$$\dot{\psi}_{max} = \frac{g}{v_t} \cos\theta \sin\phi_{max} \tag{20}$$

The guidance control laws are composed of time-constant based proportional gains. In order to achieve the desired first-order response, these time-constants must be slow enough to avoid being effected by the rate limits. Therefore, lower-limits are imposed on the time-constants by specifying the maximum errors in which the rate limits will have no effect.

$$K\tau_{\theta min} = \theta_{ERROR max} / \dot{\theta}_{max} \tag{21}$$

$$K\tau_{\phi_{min}} = \phi_{ERROR max} / \dot{\phi}_{max} \tag{22}$$

$$K\tau_{\psi_{min}} = \psi_{ERROR max} / \dot{\psi}_{max} \tag{23}$$

The maximum pitch, bank, and heading errors used for this evaluation correspond to 5 degrees, 6 degrees and 10 degrees respectively.

The actual time-constant gains are computed using frequency separation, and by taking into account the corresponding lower limits. The automatically scheduled gains are computed as follows:

$$K\tau_{\theta} = \max\left(3/\omega_q, K\tau_{\theta min}\right) \tag{24}$$

$$K\tau_{\gamma} = 3K\tau_{\theta} \tag{25}$$

$$K\tau_{h} = 3K\tau_{\gamma} \tag{26}$$

$$K\tau_{\phi} = \max\left(3/\omega_p, K\tau_{\phi_{min}}\right) \tag{27}$$

$$K\tau_{\psi} = \max\left(3K\tau_{\phi}, K\tau_{\psi_{min}}\right) \tag{28}$$

$$K\tau_{loc} = 3K\tau_{\psi} \tag{29}$$

$$K\tau_{\beta} = 3/\omega_r \tag{30}$$

Guidance Control Laws

The longitudinal guidance control laws use the automatically scheduled gains to compute FPA commands (γ_c) for each longitudinal flight mode. These commands are then converted into the associated pitch rate commands ($\dot{\theta}_c$).

The vertical speed control law uses the altitude rate command ($\dot{h}_c$) and the aircraft's ground speed (v_g) to compute

$$\gamma_c = \tan^{-1}\left(\dot{h}_c / v_g\right) \tag{31}$$

where $\dot{h}_c$ is limited to $\pm v_g \tan\gamma_{max}$.

The altitude capture and hold control law computes the altitude rate command from the altitude error (h_{err}), which is represented as the distance between the aircraft's altitude (h) and the target altitude (h_c).

$$h_{err} = h - h_c \tag{32}$$

$$\dot{h}_c = -\frac{1}{K\tau_h}\left(h_{err}\right) \tag{33}$$

The glideslope capture and tracking control law is computed similarly, however the glideslope deviation and range signals are used to compute altitude error, above or below the glideslope. The reference angle of the glideslope (γ_{ref}) is also used in order to compute

$$\dot{h}_c = v_g \tan\gamma_{ref} - \frac{1}{K\tau_h} h_{err} \tag{34}$$

The altitude and glideslope capture modes are engaged when ($h_{err} < 0$ and $\dot{h}_c < 0$) or ($h_{err} > 0$ and $\dot{h}_c > 0$).

A variable altitude flare maneuver was developed in order to accommodate a wide range of approach conditions for different aircraft. The flare control law uses the specified sink rate at touchdown ($\dot{h}_{td} < 0$) as a constant altitude rate command. The flare mode is engaged when the aircraft reaches the altitude required for the flare maneuver (h_{flare}).

$$h_{flare} = K\tau_\gamma\left(\dot{h}_{td} - v_g \tan\gamma\right) \tag{35}$$

Once the FPA command has been computed for the current longitudinal mode, the command is limited by $\pm\gamma_{max}$. The command is then converted, using FPA feedback, into the associated pitch rate command

$$\dot{\theta}_c = K\tau_\gamma\left(\gamma_c - \gamma\right) \tag{36}$$

and limited by $\pm\dot{\theta}_{max}$.

The lateral guidance control laws use the automatically scheduled gains to compute bank angle commands (ϕ_c) for each lateral flight mode. These commands are then converted into the associated roll rate commands ($\dot{\phi}_c$).

The heading select and heading hold control laws use the commanded heading angle (φ_c), and heading feedback from the aircraft's sensors (φ), to compute

$$\phi_c = \sin^{-1}\left(\frac{v_t}{g\cos\theta}\frac{1}{K\tau_\psi}\psi_{err}\right) \tag{37}$$

where the heading error

$$\psi_{err} = \psi_c - \psi \tag{38}$$

is limited to $\pm K\tau_\psi\dot{\psi}_{max}$.

The localizer capture and tracking control law is computed similarly, however the localizer deviation and range signals are used to compute the cross-track error (loc_{xtk}) from the runway centerline. The localizer reference angle (φ_{ref}) is also used in order to compute the track angle error (φ_{tke}).

$$\psi_{err} = \sin^{-1}\left(-\frac{loc_{xtk}}{v_g K\tau_{loc}}\right) - \left(\psi - \psi_{ref}\right) \tag{39}$$

where loc_{xtk} is limited to $\pm K\tau_{loc}v_g K\tau_\psi\dot{\psi}_{max}$. The localizer capture mode is engaged when ($\varphi_{err} < 0$ *and* $loc_{xtk} < 0$) or ($\varphi_{err} > 0$ *and* $loc_{xtk} > 0$).

Once the bank angle command has been computed for the current lateral mode, the command is limited by $\pm\phi_{max}$. The command is then converted, using bank angle feedback, into the associated roll rate command

$$\dot{\phi}_c = K\tau_\phi\left(\phi_c - \phi\right) \tag{40}$$

and limited by $\pm\dot{\phi}_{max}$.

Guidance Command Transformation

The guidance command transformation logic converts autopilot pitch rate and roll rate commands, into corresponding body-axis commands.

$$p_{APcmd} = \dot{\phi}_c - \dot{\psi}_c \sin\theta \tag{41}$$

$$q_{APcmd} = \dot{\theta}_c \cos\phi - \dot{\psi}_c \cos\theta \sin\phi \tag{42}$$

$$r_{APcmd} = \dot{\psi}_c \cos\theta\cos\phi - \dot{\theta}_c \sin\phi \tag{43}$$

To achieve turn coordination, the heading rate command is computed as

$$\dot{\psi}_c = \frac{g}{v_t}\sin\phi_c \cos\theta \tag{44}$$

Autopilot commands can also be transformed into normal and lateral acceleration commands.

$$nz_{APcmd} = \frac{v_t}{g}q_{APcmd} \tag{45}$$

$$ny_{APcmd} = 0 \tag{46}$$

Flight Director

Flight directors provide guidance commands to the pilot through the graphical display of pitch and bank errors. The pilot controls the pitch and bank of the aircraft in order to null the errors. A dual cue flight director uses a horizontal bar to indicate pitch error and a vertical bar to indicate bank error.

The generic flight director receives commands from the guidance control laws, and utilizes the same automatically scheduled gains. The horizontal bar is driven by the pitch error term

$$\theta_{FDe} = \left(\hat{\theta}_c - \theta\right) + \frac{K\tau_\theta}{3}\left(\dot{\theta}_c - q_f\right) \tag{47}$$

where the modified pitch command ($\hat{\theta}_c$) is rate limited by $\pm\dot{\theta}_{max}$, and the pitch rate feedback is filtered by

$$q_f = \frac{\omega_q}{s + \omega_q}q \tag{48}$$

The horizontal bar is driven by the bank error term

$$\phi_{FDe} = \left(\hat{\phi}_c - \phi\right) + \frac{K\tau_\phi}{3}\left(\dot{\phi}_c - p_f\right) \tag{49}$$

where the modified bank command ($\hat{\phi}_c$) is rate limited by $\pm\dot{\phi}_{max}$, and the roll rate feedback is filtered by

$$p_f = \frac{\omega_p}{s + \omega_p}p \tag{50}$$

Simulation Tests

The generic neural flight control and autopilot system was evaluated on high fidelity simulations of three distinctly different aircraft. A description of each simulated aircraft is provided, along with the corresponding simulator descriptions. Test results are presented, along with comparisons to each aircraft's respective conventional system.

Test Environment

Evaluations were conducted using two different flight simulation environments, figure 3. Step doublets were performed on a desktop flight simulator, which includes a generic math model and programmable flight displays.[4]

Piloted simulations were performed on the NASA Ames full-mission ACFS simulator[5]. The ACFS is equipped with a six degree-of-freedom motion system, programmable flight displays, digital sound and aural cueing system, and a 180-degree field of view visual system.

Figure 3. Desktop & Motion-Based Flight Simulators

High fidelity aerodynamic models were provided for all three simulated aircraft, which consisted of a mid-sized twin-engine commercial jet transport concept, a modified F-15 with moveable canards attached to the airframe, and a small single-engine UAV hypersonic "waverider" concept. Simulations were performed at 30 Hz for the transport, 200 Hz for the F-15, and 100 Hz for the UAV.

The Lockheed Georgia designed commercial transport concept, figure 4, is representative of a mid-size two-engine jet transport with general characteristics of a wide-body, T-tail, low wing airplane with twin turbofan engines located under the wings. The physical dimensions are similar to a Boeing 757 aircraft, and the flight characteristics of the open loop dynamics are representative of a mid-sized jet transport. This particular transport aircraft, designed as a platform for testing advanced concepts, is equipped with active flight controls representative of an advanced fly-by-wire control system.

Figure 4. Commercial Transport Concept

The F-15 ACTIVE aircraft, figure 5, is currently in operation at NASA Dryden. It is not a conventional F15 in that it has canards and thrust vectoring nozzles, which can be used to simulate failures in flight. The aircraft is configuration G of the US Air Force's Short takeoff and landing Maneuver Technology Demonstrator (S/MTD) program.

Figure 5. Modified F-15 Aircraft

The LoFLYTE™ UAV, figure 6, was developed by Accurate Automation Corporation in cooperation with NASA Langley Research Center and the US Air Force Research Laboratory at Wright-Patterson Air Force Base. The UAV is a 100 inch subsonic jet prototype of a high-lift, low-drag Mach 5 aircraft concept. It is the first flying "waverider"

airbreathing aircraft designed to “ride” the hypersonic shock wave that it produces for improved efficiency.

Figure 6. Hypersonic UAV Aircraft

The Earth atmosphere is based on a 1976 standard atmosphere model. The Dryden turbulence model is used to turbulence RMS and bandwidth values which are representative of values specified in Military Specifications Mil-Spec-8785-D of April 1989.

Test Description

The neural flight control system was evaluated on the desktop flight simulator by performing stick and rudder pedal step doublets. Results are compared to the corresponding conventional flight control system for each aircraft. While the transport and F-15 aircraft are equipped with advanced fly-by-wire control systems, the UAV is equipped with an open-loop flight control system based on actuator control.

The generic autopilot was evaluated on the desktop flight simulator using heading and vertical speed step commands, as well as altitude capture and hold maneuvers. Approach and landing scenarios were used to evaluate localizer and glideslope capture and tracking performance.

The neural flight control and flight director systems were also evaluated by NASA test pilots on the full-mission motion-based simulator. Flight tests were performed using the transport aircraft model, across multiple flight conditions under nominal and simulator failure conditions.

Test Results

The results presented in this section provide a basis for evaluating the capability, of the generic neural flight control and autopilot system, in controlling three completely different aircraft.

Figure 7 displays a sample pitch rate, roll rate, and yaw rate step doublet maneuver for the transport aircraft. The responses using the neural flight control system are compared to the transport aircraft’s conventional flight control system. The responses are similar in the pitch and roll channels. The neural flight control system demonstrates a cleaner response in the yaw channel. The yaw rate generated during the roll rate doublet is a result of turn coordination.

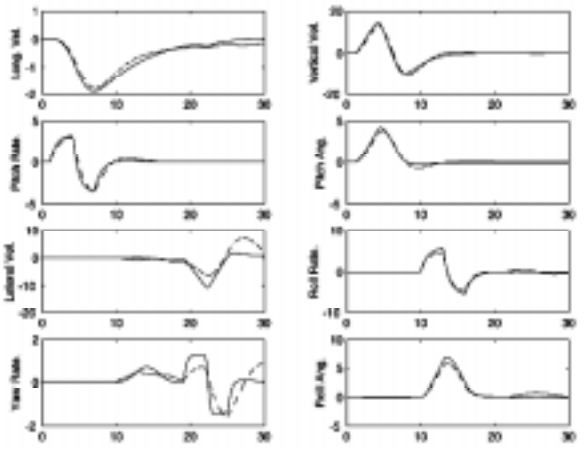

Figure 7. Transport Doublets
(- Neural, -- Conventional)

Figure 8 displays a similar step doublet maneuver for the F-15 aircraft. Once again, the responses using the neural flight control system are similar to the F-15’s conventional flight control system. The neural flight control system appears to have less coupling between the roll and yaw axes.

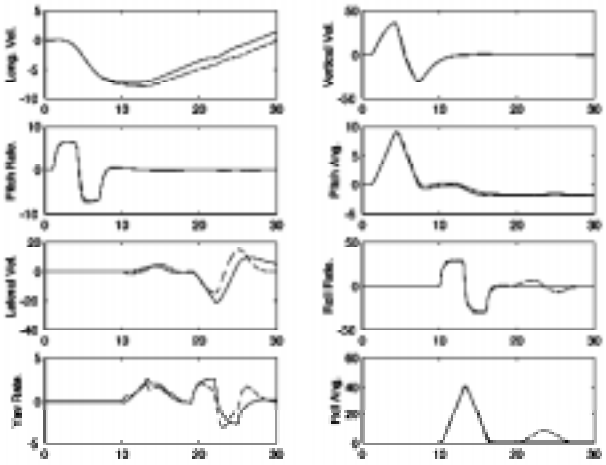

Figure 8. F-15 Doublets
(- Neural, -- Conventional)

Figure 9 displays a sample pitch rate, roll rate, and yaw rate step doublet maneuver for the UAV aircraft. Since the conventional UAV flight control system utilizes an open-loop architecture, the responses are expected to be less precise than that of a fly-by-wire control system. The pitch axis exhibits a high frequency response with a fairly large overshoot. The roll and yaw axis coupling is evident in the dutch roll oscillations.

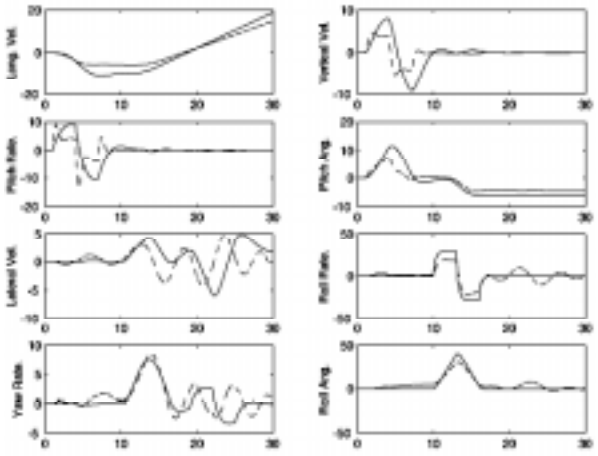

Figure 9. UAV Doublets
(- Neural, -- Conventional)

In general, the neural flight control system was found to provide a first-order response in all three axes for each aircraft. As a result, the longitudinal and lateral autopilot modes exhibited similar first-order responses. However, the generic guidance system is designed on the assumption that the neural flight control system can provide consistent handling qualities across flight conditions and under different aircraft configurations.

The neural flight control system was also evaluated by two NASA test pilots using the transport aircraft model. The handling qualities were evaluated at different flight conditions under nominal and simulated failure conditions. The simulated failures included a nose-down runaway stabilizer trim, an engine-out failure, and a controller failure. In all cases, sufficient control authority remained to stabilize the aircraft. In the case of the controller failure, the neural flight controller was initialized with no prior knowledge of the aircraft's stability and control derivatives. Essentially, the pre-trained neural network was initialized with an identity matrix for modeling the aircraft's control derivative estimates.

Under nominal conditions, the neural flight controller was described as "pure axis by axis, well damped and (with) good response". In general, it was described as "fairly representative" of the conventional controller. Under simulated failure conditions, the neural flight controller was found to provide a slight improvement over the conventional controller. In the case of the stabilizer failure, both controllers were able to automatically compensate with the elevator to stabilizer the aircraft. However the neural flight controller provided additional elevator deflection during pitch-up maneuvers, until control saturation was reached, in an attempt to provide consistent handling qualities, figure 10.

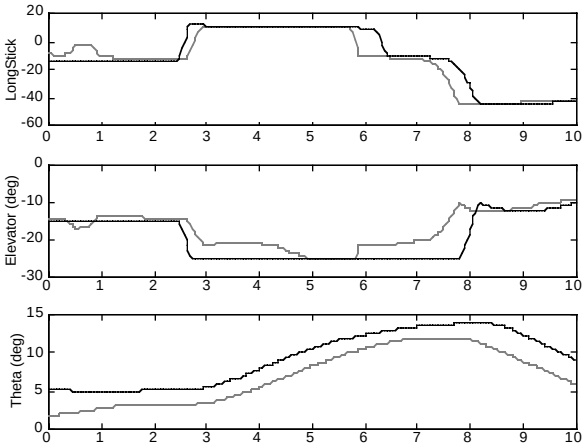

Figure 10. Stabilizer Failure
(- Neural, -- Conventional)

The neural flight controller was also able to automatically compensate for the steady-state sideslip generated by an engine-out failure, without requiring manual rudder trim, figure 11. In both failure cases, the performance under the neural flight controller was described as "transparent" to the point where "it doesn't feel like you have any problems at all".

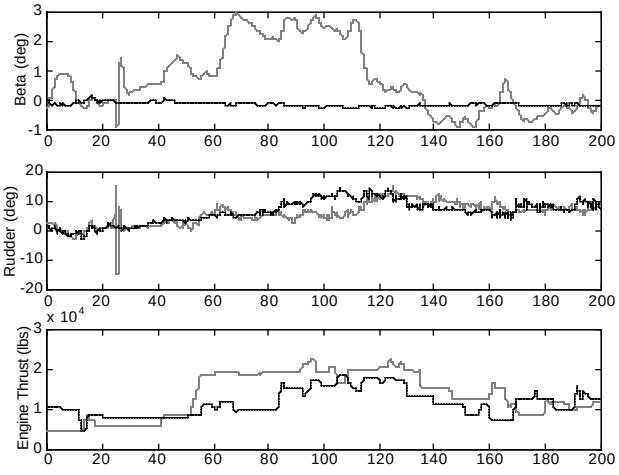

Figure 11. Engine-Out Failure
(- Neural, -- Conventional)

In the case of the controller failure, the adaptive neural networks had to perform a significant amount of adaptation, particularly in the roll channel, in order to follow desired handling quality reference models, figure 12. Pilots commented that "you can feel the handling qualities getting better…it was sloppy and then it got real precise".

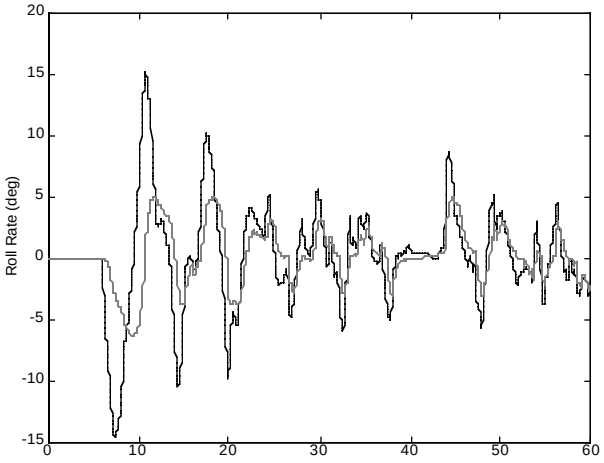

Figure 12. Controller Failure
(-- Command, - Response)

Conclusions

The neural flight control system uses pre-trained neural networks to provide dynamic estimates of the aerodynamic stability and control characteristics, which are computed using a vortex-lattice code. On-line learning neural networks are used to compensate for errors resulting from the estimates, as well as directly adapting to changes in the aircraft dynamics due to unexpected damage or failures. The generic guidance system takes advantage of the consistent handling qualities, provided by the neural flight control system, by performing automatic gain-scheduling based upon the neural flight control system's reference models.

The results presented in the previous section demonstrate the effectiveness of a generic neural flight control and autopilot system in controlling three distinctly different aircraft. The generic system can also help to reduce the high cost associated with avionics development since it does not require gain-scheduling or explicit system identification.

In general, the results demonstrate that the generic system can achieve performance, which is comparable to each aircraft's conventional system. The neural flight control system can also provide additional potential for accommodating damage or failures.

References

[1] Birch, Stuart, *Technology Update: Aircraft Data Processing*, Aerospace Engineering, August 1998.

[2] Steinberg, Marc L., *A Comparison of Intelligent, Adaptive, and Nonlinear Flight Control Laws*, AIAA 99-4044, August 1999.

[3] Rysdyk, Rolf T., and Anthony J. Calise, *Fault Tolerant Flight Control via Adaptive Neural Network Augmentation*, AIAA 98-4483, August 1998.

[4] Totah, Joseph J., David J. Kinney, John T. Kaneshige, and Shane Agabon, *An Integrated Vehicle Modeling Environment*, AIAA 99-4106, August 1999.

[5] Blake, Matthew W., *The NASA Advanced Concepts Flight Simulator: A Unique Transport Aircraft Research Environment*, AIAA-96-3518-CP.

[6] Kim, B., and Calise, A., *Nonlinear Flight Control Using Neural Networks*, AIAA Journal of Guidance, Navigation, and Control, Vol. 20, No. 1, 1997.

[7] Norgaard, M., Jorgensen, C., and Ross, J., *Neural Network Prediction of New Aircraft Design Coefficients*, NASA TM-112197, May 1997.

[8] Kaneshige, J., Bull, J., Kudzia, E., and Burcham, F., *Propulsion Control with Flight Director Guidance as an Emergency Flight Control System*, AIAA 99-3962, August 1999.